Mammal Research (2023) 68:637–646
https://doi.org/10.1007/s13364-023-00705-2

ORIGINAL PAPER

Form, function, and tissue proportions of the mustelid carnassial molar

Keegan R. Selig[1]

Received: 15 May 2023 / Accepted: 4 July 2023 / Published online: 13 July 2023

Abstract

Mustelids are an ecologically diverse group of mammals that span several dietary niches. Compared to other mammalian clades, however, less is known about how the morphology of the dentition reflects these dietary differences. The following examines dental form in the beech marten (*Martes foina*), the river otter (*Lontra canadensis*), the wolverine (*Gulo gulo*), and the sea otter (*Enhydra lutris*). Lower carnassial molar morphology is examined using methods for dental topographic analysis, enamel thickness measurement, and pulp volume measurement to assess this form-function relationship. It is predicted that mustelids will covary in their dental form with their diet, where dental topography will reflect the reliance on tough or soft foods, enamel thickness will vary as a product of hard-object feeding, and pulp volume will vary as a product of dietary abrasiveness/hard-object feeding. Results suggest that mustelid dental form reflects the dietary ecology of each species; however, pulp volume does not covary with diet as it does in anthropoid primates, for example. These animals represent a morphocline of increasing specialization in carnassial form leading from the plesiomorphic marten to the highly specialized sea otter. These results provide further evidence of convergence among mammals where molar form is largely driven by diet. These results also provide insight into how taxa such as the sea otter and wolverine are adapted to dealing with diets that include bivalves and bones, respectively, through decreased dental topography and thickened enamel.

Keywords Dental topographic analysis · Wolverine · Otter · Marten · Enamel thickness

Introduction

Among carnivorans, mustelids represent one of the most ecomorphologically diverse clades, with taxa ranging from dietary generalists (e.g., martens) to piscivores (e.g., river otters), to carrion (e.g., wolverines) and mollusk specialists (sea otters) (Law et al. 2018a). Previous research has demonstrated that mustelids differ in terms of their craniomandibular musculature (e.g., Riley 1985), their cranial form (e.g., Dumont et al. 2016; Law et al. 2018a), and their bite force (e.g., Law et al. 2018a, b; Hartstone-Rose et al. 2019) depending on diet. Mustelids also differ in terms of the form of their dentition depending on their diet based on quantitative and meristic traits (Riley 1985; Popowics 2003). Riley (1985) argued that modifications to the cheek teeth represent the most striking difference among the jaw morphologies of modern mustelids (i.e., *Martes*, *Enhydra*, *Lontra*), with a shift towards grinding in taxa such as *Enhydra*. Popowics (2003) examined mustelid postcanine dimensions and found that *Gulo gulo* favors high levels of carnassial shearing on the lower first molar (m1), whereas *E. lutris* is characterized by an emphasis on crushing instead. The metaconid in these taxa is absent or reduced respectively, which contributes to the shearing adaptation of their carnassial. *Martes* and *Lontra canadensis* have lower molars that emphasize both carnassial and transverse shearing (transverse shearing surface provided by the presence of the metaconid), while also being adapted for crushing (Popowics 2003).

The relationship between dental form and function has been studied in great detail among extant primates and other closely related taxa (e.g., Butler 1963; Kay 1975; Kay and Hylander 1978; Boyer 2008; Bunn et al. 2011; Winchester et al. 2014; Selig et al. 2019). However, comparatively little research has aimed at examining the form-function relationship of the dentition and diet among extant mustelids,

Communicated by: Jan M. Wójcik

✉ Keegan R. Selig
keegan.selig@duke.edu

[1] Department of Evolutionary Anthropology, Duke University, Durham, NC, USA

particularly in light of increased reliance on three-dimensional methods for studying the dentition. Recently, Waldman et al. (2023) examined the dental topography in a sample of living carnivorans and suggest that dental topography is indeed reflective of diet in this group, though they did not examine patterns of dental form among mustelids specifically. Moreover, Waldman et al. (2023) only sampled one individual for each species included, they examined all postcanine teeth as a single mesh or unit rather than looking at individual teeth as is more traditional in dental topographic analyses (DTA, see below), and they did not consider interspecific patterns of mustelid dental topography in their analysis. Here, DTA methods are employed, as well as methods for measuring enamel thickness and pulp volume to assess the form-function relationship of the carnassial m1 in a sample of four extant mustelid species: the wolverine (*G. gulo*), the beech marten (*M. foina*), the river otter (*L. canadensis*), and the sea otter (*E. lutris*).

Previous studies have examined the dental adaptations and morphology of mustelids (e.g., Riley 1985; Wolsan et al. 1985; Wolsan 1988; Popowics 2003; Constantino et al. 2011; Hopkins et al. 2022; Waldman et al. 2023); however, research is lacking concerning the suite of dental adaptations these animals exhibit in light of their differing diets. Moreover, most studies of extant mammalian dental form concern primates, but the degree that those patterns observed among primates converge with those of mustelids is currently unclear. The relationship between dental form and diet in mustelids is hypothesized here to be convergent with those of primates, where hard-object feeding, adaptations for resisting dental wear, and proportions of soft or tough foods consumed are manifest in the form of the molars.

The taxa included in the present study differ in terms of their dietary behaviors according to the available literature (Table 1). *Martes foina* is traditionally viewed as generalist omnivore, consuming a diet of fruit, insects, birds, and carrion. Though compared to other species of *Martes*, *M. foina* is described as being perhaps more highly reliant on fruit (Bakaloudis et al. 2012). Popowics (2003) describes the diet of *Martes* as being comprised largely of tough, soft tissue, with the addition of soft materials in their consumption of fruit. *Gulo gulo* is much more carnivorous, with the majority of the diet being comprised of animal tissue. They also are known to crack and consume large bones, with bones making up the majority of the material recovered in their scat (van Dijk et al. 2007). Popowics (2003) describes the diet of *Gulo* as being made up of tough, soft tissue, as well as hard, brittle bone. *Lontra canadensis* is another highly carnivorous species, with the majority of the diet made up of fish, though the makeup of the river otter diet varies seasonally and geographically, with some populations consuming larger quantities of crustaceans and/or mollusks (Roberts et al. 2008). Popowics (2003) describes the diet of *Lontra* as being made predominantly of soft tissue (i.e., fish). Finally, *E. lutris* is largely a hard-object feeder as this animal consumes large quantities of bivalves and sea urchins that are cracked open with their teeth. Although sea otters have been observed cracking invertebrate prey using rocks or other hard object (Fujii et al. 2017), this behavior varies significantly between populations and between individuals, with individuals using tools to crack food items between 0 and 98% of prey captures (Fujii et al. 2017). This behavior therefore likely has little effect on the dental morphology observed in *E. lutris* as a species. Popowics (2003) describes the diet of *Enhydra* as being largely made up of hard, brittle exoskeletons.

It has been suggested that *Martes* is the most plesiomorphic extant mustelid, most closely resembling the omnivorous ancestral form, being characterized by a carnassial molar that is adapted for both shearing and crushing (Riley 1985). In examining their masticatory musculature and molar form, Riley (1985) suggested that a hypothetical

Table 1 Diet by taxon with references for each taxon. Food mechanical properties are adapted from Popowics (2003)

Taxon	Diet	Food mechanical properties	References
Martes foina	Fruit, insects, birds, reptiles, carrion. Commonly regarded as generalists. Some populations may be highly frugivorous	Tough soft tissue, soft materials	Delibes 1978; Amores 1980; Rasmussen and Madsen 1985; Skírnisson 1986; Romanowski and Lesiński 1991; Clevenger 1994; Martinoli and Preatoni 1995; Popowics 2003; Bakaloudis et al. 2012
Gulo gulo	Small (rodents) to large (moose) animal prey, carrion, bone	Tough soft tissue, hard and brittle bone	Myhre and Myrberget 1975; Hornocker and Hash 1981; Popowics 2003; van Dijk et al. 2007; Koskela et al. 2013
Lontra canadensis	Predominantly fish, some insects, mollusks, crustaceans	Soft tissue	Larsen 1984; Reid et al. 1994; Popowics 2003; Roberts et al. 2008; Day et al. 2015
Enhydra lutris	Bivalves, sea urchins, crabs, kelp	Hard, brittle exoskeletons	Ostfeld 1982; Kvitek et al. 1993; Laidre and Jameson 2006; Fujii et al. 2017

lineage or morphocline from a land-dwelling omnivore to an extremely specialized aquatic sea otter can be represented from *Martes* to *Lontra* to *Enhydra*. I also considered the morphologies of these taxa to be stereotypical of the morphological stages connecting the ancestral mustelid condition with the derived condition of *Enhydra* on the one hand and *Gulo* on the other. While previous study has examined the transition from a generalized omnivore m1 to a dietary specialist (i.e., molluscivore) in this group of animals (e.g., Riley 1985), there has been no examination of three-dimensional tooth form or considerations of enamel thickness or other tissue proportions. Given that these animals split relatively recently (Fig. 1) and they differ in dietary ecology, they represent good model taxa for examining how phenotypic change may manifest given different ecologies among closely related taxa.

Variation in molar enamel thickness is commonly invoked as being related to differences in diet as thick enamel is thought to help teeth withstand the stress of hard and tough-object feeding (Dumont 1995; Lambert et al. 2004; Smith et al. 2005; Lucas et al. 2008; Braga et al. 2010; Constantino et al. 2011; Daegling et al. 2011). To date, variation in molar enamel thickness has not been examined among mustelids, with the exception of *Enhydra* (Constantino et al. 2011). Consistent with findings in extant primates, it is predicted that the hard-object feeding and bone cracking *Enhydra* and *Gulo* will be characterized by relatively thicker enamel compared to *Lontra* and *Martes*, whose molar enamel is theoretically subjected to less stress. Although *Enhydra* is characterized as having relatively thin enamel compared to modern humans (Constantino et al. 2011), it is still predicted that they will have thick enamel compared to other mustelids given their hard-object diet.

Finally, relative pulp volume has also been studied among extant primates (Selig et al. 2021a). Dental pulp helps in the maintenance and upkeep of dentine during life, and under the process of dental wear, helps in the deposit of tertiary dentine (Hamner III et al. 1964; Blumberg et al. 1971; Hillson 1996). Previous work has demonstrated that primates that consume a more abrasive diet that are consequently subject to greater dental wear, such as the hard-object feeding tufted capuchin (*Sapajus apella*) and the white-faced saki (*Pithecia pithecia*), have higher relative pulp volumes compared to closely related, more soft-object feeding taxa. It is therefore predicted that *Enhyra* and *Gulo* will be characterized by a higher relative pulp volume compared to the other taxa in the current analysis. This research will not only shed light on the dental adaptations of ecologically distinct animals, but will provide a framework for reconstructing diet in extinct mustelids as well.

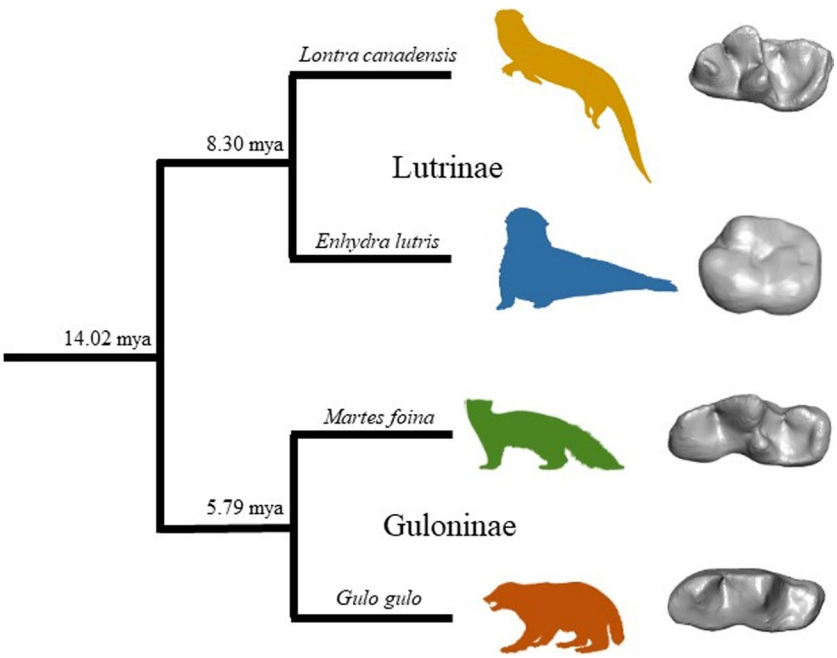

Fig. 1 Relationships and divergence dates of the included taxa based on the phylogeny of Law et al. (2018b). Representative molars of *Lontra* (UAM:87–138-112), *Enhydra* (AMNH:MAMMALS:M-24186[reversed]), *Martes* (USNM:MAMMALS:173305[reversed]), and *Gulo* (AMNH:MAMMAL:M-165766) are not to scale. Silhouettes are from phylopic.org: *Lontra* and *Enhydra* courtesy of Margot Michaud (https://www.phylopic.org/images/dd5b2173-0ed5-47e7-90e5-f501dd231ae1/lontra-felina, https://www.phylopic.org/images/d3a78afb-1b9e-45e0-b6f4-144d79f399f0/enhydra-lutris), *Martes* courtesy of Ferran Sayol (https://www.phylopic.org/images/7f7431c6-8f78-498b-92e2-ebf8882a8923/martes-foina), and *Gulo* courtesy of Steven Traver (https://www.phylopic.org/images/1f9bbb79-f060-47c1-9954-ea78812d3b91/gulo-gulo-gulo)

Materials and methods

The sample

The specimens included in the sample are summarized in Table S1. All specimens were downloaded as micro-CT scan TIF stacks from MorphoSource (Boyer et al. 2016). Scans were reconstructed and analyzed in Avizo 8.1.1 (Visualization Sciences Group 2009). The sample includes four specimens of *M. foina*, four specimens of *G. gulo*, five specimens of *L. canadensis*, and three specimens of *E. lutris*. Only specimens with unworn to lightly worn m1s were included to avoid the confounding effects of wear, thus limiting the number of specimens that could be included.

Dental topographic analysis

Three dental topographic metrics were measured (Fig. 2). Surface curvature was measured using Dirichlet normal energy (DNE) (Bunn et al. 2011; Winchester et al. 2014; Pampush et al. 2016b; Winchester 2016). This metric is measured as the degree to which a surface deviates from being planar, capturing the level of curvature or sharpness of a surface. Taxa characterized by molars with high DNE have tall, sharp teeth, which is typically associated with consuming mechanically complex or tough foods such as leaves or insects/animal tissues (e.g., Bunn et al. 2011; Ledogar et al. 2013; Winchester et al. 2014; Pampush et al. 2016a, 2018; Selig et al. 2019, 2021b; López-Aguirre et al. 2022). Second, occlusal functional composition (sometimes described as surface complexity) was measured using three-dimensional orientation patch count rotated (3D-OPCR), which estimates the number of occlusal facets based on the number of discrete patches shared by adjacent polygons on a surface (Evans et al. 2007; Winchester 2016). Molars with more cusps, crests, and ridges have higher 3D-OPCR values and tend to be more characteristic of herbivores and insectivores, whereas low 3D-OPCR values tend to correlate with the simpler molars observed in frugivores, faunivores, and carnivores (Evans et al. 2007; Winchester et al. 2014; Selig et al. 2019; López-Aguirre et al. 2022). Omnivores tend to be intermediate between the two extremes. The third DTA metric was the relief index (RFI), which is a relative measure of crown height (Ungar and M'Kirera 2003; M'Kirera and Ungar 2003; Boyer 2008) calculated as the ratio of the crown area divided by the planimetric footprint of the occlusal plane of the tooth. This metric therefore reflects how tall a tooth is relative to its footprint, meaning teeth with tall crests and ridges, or tall teeth overall, have higher RFI values. Higher RFI values have been shown to reflect reliance on insects or on other animal tissues (Boyer 2008; Selig et al. 2019; López-Aguirre et al. 2022).

Scans were segmented using Avizo 8.1.1 (Visualization Sciences Group 2009) to remove adjacent teeth. Segmented surfaces were cropped along the cervix to isolate the crown of each molar, were simplified to 10,000 faces, and smoothed 100 iterations with the lambda set at 0.6 (e.g., Boyer 2008; Bunn et al. 2011; Prufrock et al. 2016). Cropped meshes were imported into MorphoTester 1.1.1 (Winchester 2016) to measure DNE, 3D-OPCR, and RFI. The default settings for the measurement of DNE were used, with implicit fairing disabled and outlier removal percentile set at 99.9%, while the minimum patch size for 3D-OPCR was set to five polygons following Winchester (2016). Relief index was calculated as the simple ratio of the surface area of the crown to the surface area of the tooth projected on a parallel plane of the occlusal surface (Winchester 2016).

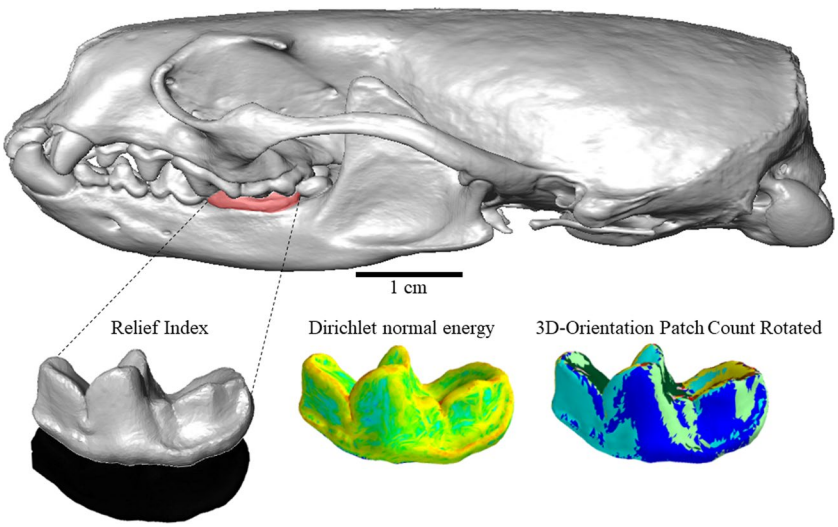

Fig. 2 Reconstruction of the skull of *Lontra canadensis* (UCLA:MAMMALS:18958) with the carnassial molar highlighted in red. Meshes representing each topographic variable are shown blown up along side the skull

Average enamel thickness

Average enamel thickness was measured following the protocol outlined by Smith et al. (2005) and was calculated as the area of the enamel divided by the length of the enamel-dentine junction (EDJ) (Fig. 3). To take these measurements, each tooth was virtually sectioned with Avizo using the "slice" module. A slice was placed through the paraconid and protoconid perpendicular to the occlusal plane. Slices were rendered using interpolation and a user-defined texture map resolution of 4096 × 4096. An image of that slice was then opened in ImageJ 1.53 and scaled. The area of the enamel (mm^2) was measured using the freehand selection tool, whereas the length of the EDJ (mm) was measured using the freehand line tool.

Percent of tooth that is pulp (PTP)

The PTP (Fig. 4) was measured following the protocol outlined by Selig et al. (2021a) using Avizo. First, the hard tissues (enamel and dentine) were segmented using threshold-based and then manual approaches. The hard tissue was segmented as a single label field and measured using the "Surface Area Volume" module to calculate the volume of these tissues. Next, the pulp cavity was then segmented as an endocast, which was also measured using the "Surface Area Volume" module in Avizo. A consistent brightness/contrast setting was used when segmenting each scan to keep baseline thresholds the same throughout the stack, while a consistent threshold range was kept throughout each individual stack. The PTP was calculated as the volume of pulp (mm^3) divided by the volume of the hard tissue, which was then multiplied by 100 to determine the percent of the total tooth volume represented by pulp.

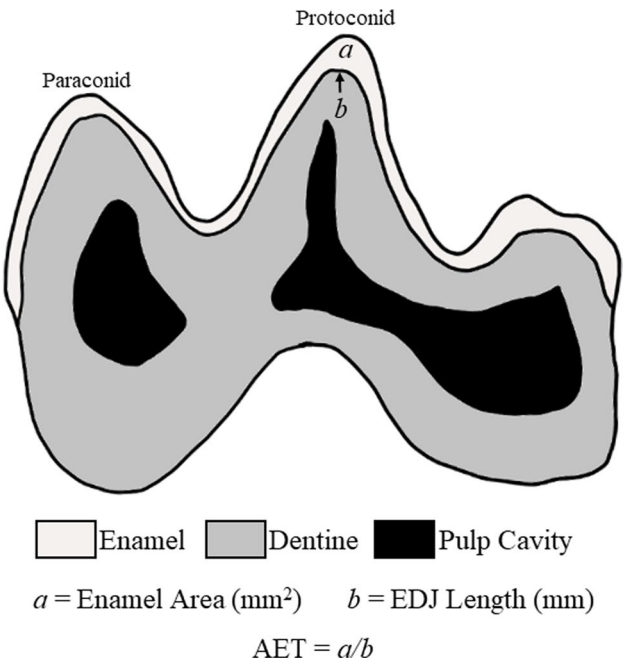

Fig. 3 Representative illustration of a lower m1 of *Lontra canadensis* showing how average enamel thickness (AET) was calculated as the area of the enamel divided by the length of the enamel-dentine junction (EDJ) from a slice taken through the paraconid and protoconid

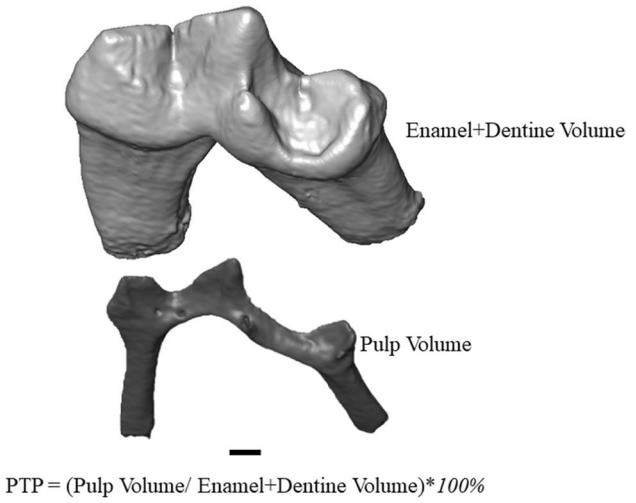

Fig. 4 Reconstruction of the m1 of *Lontra canadensis* (UAM:87–138-103) demonstrating how the percent of tooth that is pulp (PTP) was measured. Scale = 1 mm

Statistical analysis

Data were plotted in boxplots to visualize the range of variation of each variable for each included taxon. All statistical tests were performed using PAST 4.03 (Hammer et al. 2001). The Kruskal–Wallis (non-parametric ANOVA) test was used to compare medians of each metric. In cases where the Kruskal–Wallis was significant, pairwise Dunn's post hoc tests were used to determine which taxa differ from one another based on each metric. The Bonferroni correction was used for each Dunn's post hoc test. Finally, a principal component analysis (PCA) was performed to visualize variation and better understand which variables explain a greater portion of the variation. The correlation matrix was used for the PCA to remove the effect of scale from non-scaled variables. Only those axes that explained more than 25% of the total variation were considered in the PCA.

Results

Results for each metric are summarized in Table 2 and in Fig. 5. Results of the Kruskal–Wallis are summarized in Table 3 and suggest that there are significant differences between sample medians based on each metric except for

Table 2 Mean, standard deviation (Stand. Dev), and the coefficient of variation (Coeff. Var) for the measurement of Dirichlet normal energy (DNE), three-dimensional orientation patch count rotated (3D-OPCR), relief index (RFI), average enamel thickness (AET), and the percent of tooth that is pulp (PTP). Sample size indicated in brackets for each taxon

		Lontra canadensis (5)	*Enhydra lutris* (3)	*Martes foina* (4)	*Gulo gulo* (4)
DNE	Mean	354.095	143.928	231.865	192.406
	Stand. Dev	54.065	14.973	32.468	21.106
	Coeff. Var	15.269	10.403	14.003	10.970
3D-OPCR	Mean	73.900	66.083	46.813	49.219
	Stand. Dev	5.855	12.331	2.530	12.692
	Coeff. Var	7.923	18.660	5.405	25.790
RFI	Mean	2.522	1.874	2.579	2.230
	Stand. Dev	0.131	0.107	0.147	0.175
	Coeff. Var	5.195	5.731	5.691	7.861
AET	Mean	0.249	0.625	0.231	0.406
	Stand. Dev	0.032	0.087	0.028	0.061
	Coeff. Var	12.754	13.864	11.966	15.090
PTP	Mean	9.034	7.788	9.566	7.275
	Stand. Dev	1.951	2.230	7.094	6.064
	Coeff. Var	21.600	28.629	74.153	83.360

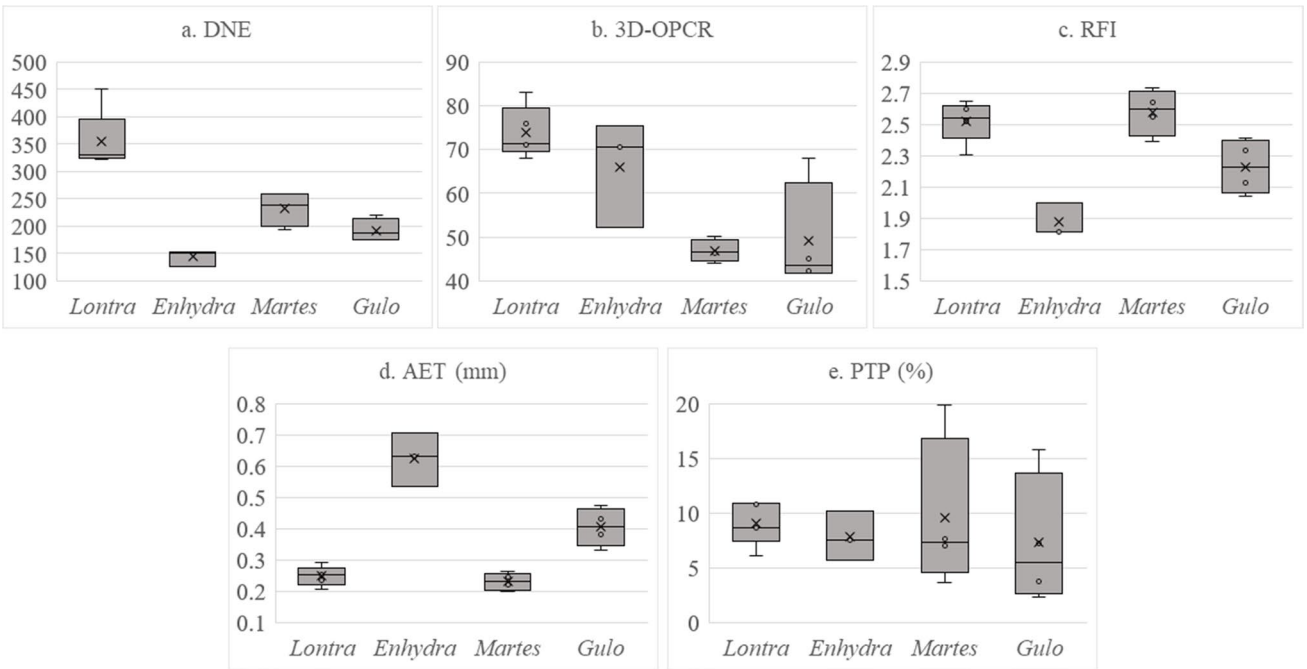

Fig. 5 Boxplots showing the results of the measurement of Dirichlet normal energy (DNE), three-dimensional orientation patch count rotated (3D-OPCR), relief index (RFI), average enamel thickness (AET), and the percent of tooth that is pulp (PTP). The X denotes the mean, the horizontal lines denote the median, the boxes represent the upper and lower quartiles, and whiskers denote the highest and lowest values for each taxon

PTP. Results of the Dunn's post hoc tests are summarized in Table 4. Based on the measurement of DNE, *Lontra* has the most highly curved teeth and has significantly higher DNE than *Enhydra*, which has the lowest DNE. There is more overlap and greater intraspecific variation in the measurement of 3D-OPCR, with *Gulo* and *Lontra* differing form one another significantly. Generally speaking, the lutrines have higher molar complexity than the gulonines. Based on the measurement of RFI, *Enhydra* has the lowest relief, whereas *Martes* has the highest, with this difference being significant. *Gulo* and *Lontra* are both intermediate in their RFI. The taxon with the highest AET, and therefore the

Table 3 Results of the non-parametric Kruskal–Wallis test for each metric. *DNE* Dirichlet normal energy, *3D-OPCR* three-dimensional orientation patch count rotated, *RFI* relief index, *AET* average enamel thickness, *PTP* percent of tooth that is pulp. Bolded values are significant

Metric	$H(chi^2) =$	$P =$
DNE	13.17	**0.0043**
3D-OPCR	10.74	**0.0131**
RFI	10.69	**0.0135**
AET	12.22	**0.0067**
PTP	1.72	0.6319

thickest enamel, was *Enhydra* followed by *Gulo*. *Enhydra* has significantly higher AET than both *Martes* and *Lontra*. Finally, there is very little variation in PTP. *Lontra* generally has the highest PTP, followed by *Enhydra*, *Martes*, and then *Gulo*, but these differences are not significant.

The first two axes of the PCA are plotted in Fig. 6. The eigenvalues and percent variance explained by each principal component, as well as the loadings for each variable, are summarized in Table 5. Along component 1, DNE, RFI, and AET explain most of the variation, with *Lontra* plotting in positive morphospace due to their high DNE and RFI, and low AET, whereas *Enhydra* plots in negative morphospace due to their high AET, and low DNE and RFI. *Martes* plots in more intermediate morphospace, near *Lontra*, likely due to their high *RFI*, whereas *Gulo* plots in more negative morphospace due to having relatively low DTA measures and thick enamel. Along component 2, 3D-OPCR explains the majority of the variation. This axis does not separate taxa as clearly as along component 1, but does distinguish *Martes* from *Enhydra* and *Lontra* given the low molar complexity of *Martes*. *Gulo* sits in intermediate morphospace along this axis.

Discussion

These results are generally consistent with previous findings in that mustelid molar form varies as a product of dietary ecology, a pattern convergent with living primates (e.g., Butler 1963; Kay 1975; Kay and Hylander 1978; Boyer 2008; Bunn et al. 2011; Winchester et al. 2014; Selig et al. 2019). These results also support the notion that dental topography is reflective of diet among carnivorans (Waldman et al. 2023). However, these results provide new insight into more nuanced means of variation in carnassial form among mustelids.

Martes is described as being highly pleiomorphic in molar form, with a carnassial molar adapted for shearing and crushing foods (Riley 1985). The high RFI, intermediate DNE, and low 3D-OPCR exhibited by this taxon likely reflects the long, yet simple shearing crests present on the carnassial. *Martes* is characterized by relatively thin enamel, likely as a result of the animal consuming very few hard foods relative to *Enhydra* or *Gulo*. If the carnassial molar of *Martes* is viewed as the starting point in the morphocline examined herein, *Gulo* may be next in the evolution of more highly specialized molars. *Gulo* is characterized by a suite of dental features that are similar to those of *Martes*, with intermediate DNE and low complexity. However, *Gulo* is characterized by thicker enamel and lower RFI, likely reflecting the bone cracking behavior observed in wolverines. Both *Martes* and *Gulo* are characterized as consuming tough, soft tissue (Popowics 2003), which may explain their similar dental topographic values.

The lower first molar of *Lontra* still maintains the carnassial bauplan observed in *Martes*, but is characterized by a more distinctive suite of adaptations. For example, *Lontra* has generally high topographic values, reflecting their sharp and complex shearing crests, which likely aid in capturing and processing soft, slippery fish. *Lontra* is characterized by thin enamel, as with *Martes*. However, observational work suggests that *Lontra* consumes at least some prey items that could be considered "hard," such as mollusks or crustaceans, which may make up large portions of the diet seasonally (Roberts et al. 2008). The finding of thin enamel is somewhat unexpected considering both *Gulo* and *Enhydra* have thick

Table 4 Bonferroni-corrected Dunn's post hoc tests for each metric that varied significantly as per the Kruskal–Wallis (see Table 3). Bolded values are significant

Metric		*Lontra canadensis*	*Enhydra lutris*	*Martes foina*
DNE	*Enhydra lutris*	**0.003347**	–	–
	Martes foina	0.6013	0.3805	–
	Gulo gulo	0.09144	1	1
3D-OPCR	*Enhydra lutris*	1	–	–
	Martes foina	0.08342	0.6813	–
	Gulo gulo	**0.02952**	0.3509	1
RFI	*Enhydra lutris*	0.05784	x	–
	Martes foina	1	**0.02329**	–
	Gulo gulo	0.8216	1	0.3803
AET	*Enhydra lutris*	**0.04116**	–	–
	Martes foina	1	**0.01868**	–
	Gulo gulo	0.3882	1	0.1876

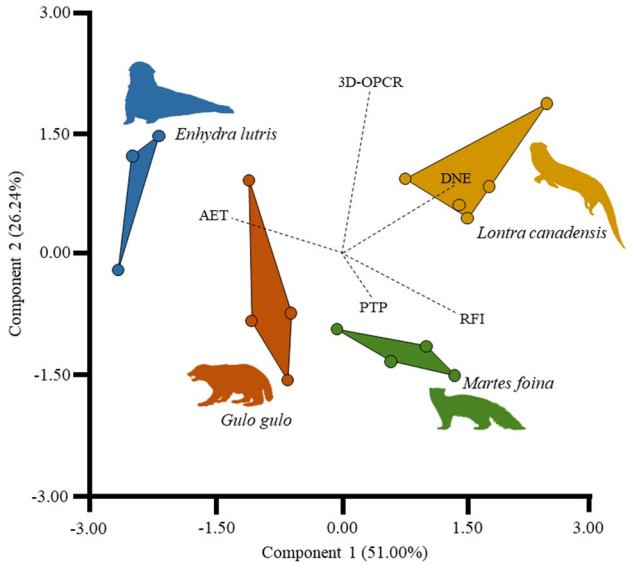

Fig. 6 Plot of the first two principal components depicting where each taxon sits in the morphospace. Variance explained by each PC is in brackets. The biplots indicate how Dirichlet normal energy (DNE), three-dimensional orientation patch count rotated (3D-OPCR), relief index (RFI), average enamel thickness (AET), and the percent of tooth that is pulp (PTP) are loaded along these two axes. Silhouettes are from phylopic.org: *Lontra* and *Enhydra* courtesy of Margot Michaud (https://www.phylopic.org/images/dd5b2173-0ed5-47e7-90e5-f501dd231ae1/lontra-felina, https://www.phylopic.org/images/d3a78afb-1b9e-45e0-b6f4-144d79f399f0/enhydra-lutris), *Martes* courtesy of Ferran Sayol (https://www.phylopic.org/images/7f7431c6-8f78-498b-92e2-ebf8882a8923/martes-foina), and *Gulo* courtesy of Steven Traver (https://www.phylopic.org/images/1f9bbb79-f060-47c1-9954-ea78812d3b91/gulo-gulo-gulo)

Table 5 Eigenvalue and percent of total variance explained by each principal component. Loading coefficients for each variable included in the principal component analysis

	PC 1	PC 2	PC 3	PC 4	PC 5
% Variance	50.998	50.998	50.998	50.998	50.998
Eigenvalue	2.550	2.550	2.550	2.550	2.550
DNE	0.562	0.355	0.017	0.317	−0.676
3D-OPCR	0.139	0.833	0.175	−0.169	0.478
RFI	0.571	−0.301	−0.047	0.519	0.558
AET	−0.562	0.194	0.267	0.759	−0.003
PTP	0.151	−0.223	0.946	−0.163	−0.048

enamel associated with their diet, whereas *Lontra* does not. What's more is the pattern of carnassial topography observed in *Lontra* is very much unlike that of *Enhydra*, which is characterized by a significant reduction in crests and cusp height. Although *Lontra* consumes some similar hard food items, clearly the selective pressures for teeth adapted to process soft fish tissue were greater than those for resisting dental wear or damage from the consumption of hard prey. *Enhyrda* is characterized by relatively thin enamel compared to humans, but has enamel microstructure that is thought to help resist wear and damage (Constantino et al. 2011). Perhaps enamel microstructure in *Lontra* also helps this animal resist wear and damage, while maintaining sharp shearing blades associated with piscivory. Research into dental damage, such as enamel chipping (e.g., Fannin et al. 2020; Towle and Loch 2021), may also provide further insight into the apparent evolutionary tradeoff in the carnassial molars of *Lontra.*

The carnassial molars of *Enhydra* are also characterized by a relatively unique suite of dental features compared to the plesiomorphic *Martes*, as well as the other included mustelids; *Enhydra* has low curvature (DNE) and relief (RFI), and very thick enamel. Certainly, these adaptations reflect the reliance on hard, brittle prey items such as clams. This reduction in shearing crests and cusp height is convergent on what is observed among hard-object feeding primates such as bearded sakis (*Chiropotes*) or mangabeys (*Cercocebus* and *Lophocebus*) (Ledogar et al. 2013; Avià et al. 2022). *Enhydra*, therefore, represents an extreme on the spectrum of carnassial evolution among mustelids, showing a high degree of specialization and a shift towards crushing and grinding and away from the carnassial shear observed in *Martes* (Riley 1985).

Previous work demonstrated that anthropoid primates that consume a hard/abrasive diet are characterized by a higher relative volume of molar pulp compared to closely related taxa with softer diets (Selig et al. 2021a). This phenomenon is thought to reflect the fact the dental pulp provides, in essence, the raw material for the deposition of tertiary dentine, which helps teeth resist wear. It was predicted here that *Gulo*, and certainly *Enhydra*, would be characterized by a relatively higher volume of pulp compared to *Lontra* and *Martes*, which consume lower volumes of hard or abrasive foods. The results of the current study do not support this hypothesis, finding no significant differences in pulp volume among the selected taxa, with *Martes* and then *Lontra* characterized by the highest mean PTP. It could be argued that both *Martes* and *Lontra* also consume a hard or abrasive diet in that *Martes* crushes the bones of the small prey that it consumes (birds and reptiles), and that *Lontra* consumes high volumes of hard and brittle crustaceans. However, given the other suite of dental features examined here, it is surprising to see no evidence of adaptations for resisting wear via high pulp volumes when carnassial topography and enamel thickness clearly reflect this dietary component in *Gulo* and *Enhydra.* Perhaps thick enamel, or even enamel microstructure (Constantino et al. 2011), provides enough resistance among mustelid carnassials such that there has been little to no adaptive pressure to increase the store of pulp. Moreover, variation in PTP among anthropoids may be apomorphic among this group. More research into variation in molar pulp volume among mammals is clearly needed to fully understand this adaptation.

Although previous research has demonstrated that mustelid dental topography varies as a product of diet (Waldman et al. 2023), the present study may provide a more directly applicable means for reconstructing diet in the mustelid fossil record. Indeed, much of the mammalian fossil record is comprised of isolated teeth, meaning comparative studies concerning single teeth may be more useful compared to those that examine the entire toothrow. Considering the degree of variation in the lower m1 observed in the present study, this tooth position in particular seems to be useful in discerning diet and will likely provide insight into the dietary adaptations of extinct mustelids.

Supplementary Information The online version contains supplementary material available at https://doi.org/10.1007/s13364-023-00705-2.

Acknowledgements I would like to thank Caitlin Yoakum and Laurel Lamb for access to the UAM specimens. Blaire Van Valkenburgh and Tim Rowe provided access to the UCLA specimens and USNM:MAMMALS:157327 and USNM:MAMMALS:314885, with data collection funded by NSF IOB-0517748 and data upload to MorphoSource funded by DBI-1902242. AMNH:MAMMALS:M-24186 was provided by the authors of Tseng ZJ, Grohé C, Flynn JJ. 2016. *A unique feeding strategy of the extinct marine mammal Kolponomos: convergence on sabretooths and sea otters*. Proceedings of the Royal Society B: Biological Sciences, the collection of which was funded by the National Science Foundation (DEB-1257572) and the American Museum of Natural History Frick Postdoctoral Fellowships. All specimens were downloaded from MorphoSource.org, Duke University. I would like to thank the staff of MorphoSource for all of their tireless work to keep these data available for scientists around the world.

Data Availability All data included in this study are available in the Supplemental Table, or by request.

Declarations

Ethical approval No live animals were used in this study; therefore, no ethical approval was necessary.

Competing interests The author declares no competing interests.

References

Amores F (1980) Feedings habits of the stone martens, *Martes foina* (Erxleben, 1777), in south western Spain. Saugetierkundliche Mitteilungen 28:316–322

Avià Y, Romero A, Estebaranz-Sánchez F et al (2022) Dental topography and dietary specialization in Papionini primates. Front Ecol Evol 10:969007

Bakaloudis DE, Vlachos CG, Papakosta MA et al (2012) Diet composition and feeding strategies of the stone marten (*Martes foina*) in a typical Mediterranean ecosystem. Sci World J 2012:163920

Blumberg JE, Hylander WL, Goepp RA (1971) Taurodontism: a biometric study. Am J Phys Anthropol 34:243–255

Boyer DM (2008) Relief index of second mandibular molars is a correlate of diet among prosimian primates and other euarchontan mammals. J Hum Evol 55:1118–1137

Boyer DM, Gunnell GF, Kaufman S, McGeary TM (2016) MorphoSource: archiving and sharing 3-D digital specimen data. Paleontol Soc Pap 22:157–181

Braga J, Thackeray JF, Subsol G et al (2010) The enamel–dentine junction in the postcanine dentition of *Australopithecus africanus*: intra-individual metameric and antimeric variation. J Anat 216:62–79

Bunn JM, Boyer DM, Lipman Y et al (2011) Comparing Dirichlet normal surface energy of tooth crowns, a new technique of molar shape quantification for dietary inference, with previous methods in isolation and in combination. Am J Phys Anthropol 145:247–261

Butler PM (1963) Tooth morphology and primate evolution. In: Brothwell DR (ed) Dental anthropology. Symposium of the Society for the Study of Human Biology. Pergamon Press, New York, pp 1–13

Clevenger AP (1994) Feeding ecology of Eurasian pine marten *Martes martes* and stone marten *Martes foina* in Europe. In: Buskirk S, Harestad A, Raphael M, Powell R (eds) Martens, sables and fishers: biology and conservation. Comstock Publishing Associates, New York, pp 326–340

Constantino PJ, Lee JJ-W, Morris D et al (2011) Adaptation to hard-object feeding in sea otters and hominins. J Hum Evol 61:89–96

Daegling DJ, McGraw WS, Ungar PS et al (2011) Hard-object feeding in sooty mangabeys (*Cercocebus atys*) and interpretation of early hominin feeding ecology. PLoS One 6:e23095

Day CC, Westover MD, McMillan BR (2015) Seasonal diet of the northern river otter (*Lontra canadensis*): what drives prey selection? Can J Zool 93:197–205

Delibes M (1978) Feeding habits of the stone marten *Martes foina*, in northern Burgos, Spain. Zeitschrift Für Säugetierkunde 43:282–288

Dumont ER (1995) Enamel thickness and dietary adaptation among extant primates and chiropterans. J Mammal 76:1127–1136

Dumont M, Wall CE, Botton-Divet L et al (2016) Do functional demands associated with locomotor habitat, diet, and activity pattern drive skull shape evolution in musteloid carnivorans? Biol J Linn Soc 117:858–878

Evans AR, Wilson GP, Fortelius M, Jernvall J (2007) High-level similarity of dentitions in carnivorans and rodents. Nature 445:78–81

Fannin LD, Guatelli-Steinberg D, Geissler E et al (2020) Enamel chipping in Taï Forest cercopithecids: implications for diet reconstruction in paleoanthropological contexts. J Hum Evol 141:102742

Fujii JA, Ralls K, Tinker MT (2017) Food abundance, prey morphology, and diet specialization influence individual sea otter tool use. Behav Ecol 28:1206–1216

Hammer Ø, Harper DAT, Ryan PD (2001) PAST: paleontological statistics software package for education and data analysis. Palaeontol Electron 4(1):9

Hamner JE III, Witkop CJ Jr, Metro PS (1964) Taurodontism: report of a case. Oral Surg Oral Med Oral Pathol 18:409–418

Hartstone-Rose A, Hertzig I, Dickinson E (2019) Bite force and masticatory muscle architecture adaptations in the dietarily diverse Musteloidea (Carnivora). Anat Rec Hoboken NJ 2007 302:2287–2299

Hillson S (1996) Dental anthropology. Cambridge University Press, Cambridge

Hopkins SSB, Price SA, Chiono AJ (2022) Influence of phylogeny on the estimation of diet from dental morphology in the Carnivora. Paleobiology 48:324–339

Hornocker MG, Hash HS (1981) Ecology of the wolverine in northwestern Montana. Can J Zool 59:1286–1301

Kay RF (1975) The functional adaptations of primate molar teeth. Am J Phys Anthropol 43:195–215

Kay R, Hylander W (1978) The dental structure of mammalian folivores with special reference to primates and Phalangeroidea (Marsupialia). In: Montgomery GG (ed) The Biology of Arboreal Folivores. Smithsonian Institution Press, Washington DC, pp 173–191

Koskela A, Kojola I, Aspi J, Hyvärinen M (2013) The diet of breeding female wolverines (*Gulo gulo*) in two areas of Finland. Acta Theriol (warsz) 58:199–204

Kvitek RG, Bowlby CE, Staedler M (1993) Diet and foraging behavior of sea otters in Southeast Alaska. Mar Mammal Sci 9:168–181
Laidre KL, Jameson RJ (2006) Foraging patterns and prey selection in an increasing and expanding sea otter population. J Mammal 87:799–807
Lambert JE, Chapman CA, Wrangham RW, Conklin-Brittain NL (2004) Hardness of cercopithecine foods: implications for the critical function of enamel thickness in exploiting fallback foods. Am J Phys Anthropol 125:363–368
Larsen DN (1984) Feeding habits of river Otters in coastal southeastern Alaska. J Wildl Manag 48:1446–1452
Law C, Duran E, Hung N et al (2018a) Effects of diet on cranial morphology and biting ability in musteloid mammals. J Evol Biol 31:1918–1931
Law C, Slater G, Mehta R (2018b) Lineage diversity and size disparity in Musteloidea: testing patterns of adaptive radiation using molecular and fossil-based methods. Syst Biol 67:127–144
Ledogar JA, Winchester JM, St. Clair EM, Boyer DM (2013) Diet and dental topography in pitheciine seed predators. Am J Phys Anthropol 150:107–121
López-Aguirre C, Hand SJ, Simmons NB, Silcox MT (2022) Untangling the ecological signal in the dental morphology in the bat superfamily Noctilionoidea. J Mamm Evol 29:531–545
Lucas P, Constantino P, Wood B, Lawn B (2008) Dental enamel as a dietary indicator in mammals. BioEssays 30:374–385
M'Kirera F, Ungar PS (2003) Occlusal relief changes with molar wear in *Pan troglodytes troglodytes* and *Gorilla gorilla gorilla*. Am J Primatol 60:31–41
Martinoli A, Preatoni D (1995) Food habits of the stone marten (*Martes foina*) in the upper Aveto Valley (Northern Apennines, Italy). Hystrix Ital J Mammal 7:131–142
Myhre R, Myrberget S (1975) Diet of wolverines (*Gulo gulo*) in Norway. J Mammal 56:752–757
Ostfeld RS (1982) Foraging strategies and prey switching in the California sea otter. Oecologia 53:170–178
Pampush JD, Spradley JP, Morse PE et al (2016a) Wear and its effects on dental topography measures in howling monkeys (*Alouatta palliata*). Am J Phys Anthropol 161:705–721
Pampush JD, Winchester JM, Morse PE et al (2016b) Introducing molaR: a new R package for quantitative topographic analysis of teeth (and other topographic surfaces). J Mamm Evol 23:397–412
Pampush JD, Spradley JP, Morse PE et al (2018) Adaptive wear-based changes in dental topography associated with atelid (Mammalia: Primates) diets. Biol J Linn Soc 124:584–606
Popowics TE (2003) Postcanine dental form in the mustelidae and viverridae (Carnivora: Mammalia). J Morphol 256:322–341
Prufrock KA, López-Torres S, Silcox MT, Boyer DM (2016) Surfaces and spaces: troubleshooting the study of dietary niche space overlap between North American stem primates and rodents. Surf Topogr Metrol Prop 4:024005
Rasmussen AM, Madsen AB (1985) The diet of the stone marten *Martes foina* in Denmark. Natura Jutlandica 21:141–144
Reid DG, Code TE, Reid ACH, Herrero SM (1994) Food habits of the river otter in a boreal ecosystem. Can J Zool 72:1306–1313
Riley MA (1985) An analysis of masticatory form and function in three mustelids (*Martes americana, Lutra canadensis, Enhydra lutris*). J Mammal 66:519–528
Roberts NM, Rabeni CF, Stanovick JS, Hamilton DA (2008) River otter, *Lontra canadensis*, food habits in the Missouri Ozarks. Can Field Nat 122:303–311
Romanowski J, Lesiński G (1991) A note on the diet of stone marten in southeastern Romania. Acta Theriol 36:201–204
Selig KR, Sargis EJ, Silcox MT (2019) The frugivorous insectivores? Functional morphological analysis of molar topography for inferring diet in extant treeshrews (Scandentia). J Mammal 100:1901–1917
Selig KR, Kupczik K, Silcox MT (2021a) The effect of high wear diets on the relative pulp volume of the lower molars. Am J Phys Anthropol 174:804–811
Selig KR, Schroeder L, Silcox MT (2021b) Intraspecific variation in molar topography of the early Eocene stem primate *Microsyops latidens* (Mammalia, ?Primates). J Vertebr Paleontol 41:e1995738
Skírnisson K (1986) Untersuchungen zum Raum-Zeit System freilebender Steinmarder (*Martes foina* Erxleben, 1777). Beitr Wildbiol 6:1–200
Smith TM, Olejniczak AJ, Martin LB, Reid DJ (2005) Variation in hominoid molar enamel thickness. J Hum Evol 48:575–592
Towle I, Loch C (2021) Tooth chipping prevalence and patterns in extant primates. Am J Phys Anthropol 175:292–299
Ungar PS, M'Kirera F (2003) A solution to the worn tooth conundrum in primate functional anatomy. Proc Natl Acad Sci USA 100:3874–3877
van Dijk J, Hauge K, Landa A et al (2007) Evaluating scat analysis methods to assess wolverine *Gulo gulo* diet. Wildl Biol 13:62–67
Visualization Sciences Group (2009) AVIZO v8.1.1. Mercury Computer systems. Burlington, MA
Waldman E, Gonzalez Y, Flynn JJ, Tseng ZJ (2023) Dental topographic proxies for ecological characteristics in carnivoran mammals. J Anat 242:627–641
Winchester JM (2016) MorphoTester: an open source application for morphological topographic analysis. PLoS One 11:e0147649
Winchester JM, Boyer DM, St. Clair EM et al (2014) Dental topography of platyrrhines and prosimians: convergence and contrasts. Am J Phys Anthropol 153:29–44
Wolsan M (1988) Morphological variations of the first upper molar in the genus *Martes* (Carnivora, Mustelidae). Mém Mus Natl Hist Nat Sér C 53:241–254
Wolsan M, Ruprecht AL, Buchalczyk T (1985) Variation and asymmetry in the dentition of the pine and stone martens (*Martes martes* and *M. foina*) from Poland. Acta Theriol 30:79–114